Pressure-Driven Metal-Insulator Transition in Hematite from Dynamical Mean-Field Theory

J. Kuneš,[1,2] Dm. M. Korotin,[3] M. A. Korotin,[3] V. I. Anisimov,[3] and P. Werner[4]

[1]*Theoretical Physics III, Center for Electronic Correlations and Magnetism, Institute of Physics, University of Augsburg, Augsburg 86135, Germany*

[2]*Institute of Physics, Academy of Sciences of the Czech Republic, Cukrovarnická 10, 162 53 Praha 6, Czech Republic*

[3]*Institute of Metal Physics, Russian Academy of Sciences, 620041 Yekaterinburg GSP-170, Russia*

[4]*Theoretische Physik, ETH Zurich, 8093 Zurich, Switzerland*

(Received 16 October 2008; published 7 April 2009)

The local density approximation combined with dynamical mean-field theory is applied to study the paramagnetic and magnetically ordered phases of hematite Fe_2O_3 as a function of volume. As the volume is decreased, a simultaneous first-order insulator-metal and high-spin to low-spin transition occurs close to the experimental value of the critical volume. The high-spin insulating phase is destroyed by a progressive reduction of the spectral gap with increasing pressure, upon closing of which the high-spin phase becomes unstable. We conclude that the transition in Fe_2O_3 at ≈ 50 GPa can be described as an electronically driven volume collapse.

DOI: 10.1103/PhysRevLett.102.146402 PACS numbers: 71.30.+h, 71.27.+a, 75.50.Bb, 91.60.Gf

The metal-insulator transition (MIT) is one of the central topics in the physics of strongly correlated electron materials. Despite considerable progress in understanding of this phenomenon in the past decade, we are only starting to uncover the multitude of possible transition scenarios in real materials. An important instance of the MIT is the pressure-driven transition accompanied by a change of the local spin state [high spin (HS) to low spin (LS) transition] seen in MnO [1], $BiFeO_3$ [2], or Fe_2O_3. Understanding of the pressure-driven HS-LS transition and its relationship to the MIT and structural or volume changes is relevant to a broader class of oxides [3], often with geophysical implications.

In this Letter we study the spin and metal-insulator transition in hematite (α-Fe_2O_3) under pressure using the local density approximation combined with dynamical mean-field theory (LDA + DMFT approach) [4]. We investigate the effect of temperature and magnetic long-range order (LRO) and suggest a new classification of the simultaneous spin and metal-insulator transitions in related materials. At ambient conditions, hematite is an antiferromagnetic (AFM) insulator ($T_N = 956$ K) with the corundum structure [5]. The iron ions having a formal Fe^{3+} valence with five d electrons give rise to a local HS state. Photoemission spectroscopy (PES) [6,7] classified hematite as a charge-transfer insulator. A charge gap of 2.0–2.7 eV was inferred from the electrical conductivity data [8]. Under pressure, a first-order phase transition is observed at approximately 50 GPa (82% of the equilibrium volume) at which the specific volume decreases by almost 10% and the crystal symmetry is reduced (to the Rh_2O_3-II structure) [9–11]. The high-pressure phase is characterized by metallic conductivity and the absence of both magnetic LRO and the HS local moment [10]. Badro *et al.* showed that the structural transition actually precedes the electronic transition, which is, nevertheless, accompanied by a sizable reduction of the bond lengths [12].

Investigations of the electronic structure of hematite using various theoretical approaches lead to different (and frequently controversial) results. Similar to many transition metal oxides, the local spin density (LSDA) and generalized gradient approximations fail to reproduce the ground state under ambient conditions, severely underestimating the magnetic moment on iron and the spectral gap [13]. The static mean-field LSDA + U approach [14] improves the size of the magnetic moment and spectral gap in the HS phase, but fails to capture the metal-insulator transition; thus, LSDA appears more appropriate for the description of the LS high-pressure phase. The LDA + DMFT method, which can describe the evolution from strong to weak correlations, is well suited to study the transition regime [15]. The only DMFT study of Fe_2O_3 to date was limited to the t_{2g} band manifold finding a low-spin metallic phase at high pressure [16].

Here we use a Hamiltonian including explicitly all O-p and Fe-d orbitals, which allows us to address the following questions. (i) Is there an electronic transition without a change of the crystal structure? (ii) Is there a simultaneous metal-insulator and local moment transition as found in the isoelectronic MnO [15]? (iii) What is the nature of the transition and how is it affected by temperature and magnetic LRO? We employ the implementation of LDA + DMFT, previously applied to NiO [17], to ''solve'' the first-principles multiband Hubbard Hamiltonian

$$\hat{H} = \sum_k \hat{\mathbf{a}}_k^\dagger \mathbf{H}_k \hat{\mathbf{a}}_k - \varepsilon_{dc}(n_d)\hat{N}_d + \sum_{i\in \mathrm{Fe}} \hat{\mathbf{n}}_i^d \mathbf{U}^{dd} \hat{\mathbf{n}}_i^d$$

in the dynamical mean-field approximation. Here, $\mathbf{H}_k$ is the LDA Hamiltonian, 38×38 matrices (two Fe_2O_3 units) in the basis of Fe-d and O-p Wannier orbitals, on a uniform

k mesh in the first Brillouin zone [18]. The second term is the double-counting correction amounting to a constant shift applied to Fe-d site energies. The last term is the two-particle interaction at the Fe sites in the density-density approximation, parametrized with $U = 6.8$ eV and $J = 0.86$ eV [19]. (Fits to the PES yield U of 8 eV [6] or 7 eV [20].) We have used the double-counting correction $\varepsilon_{\rm dc} = (N_{\rm orb} - 1)\bar{U}\bar{n}_d$, previously successfully applied in the DMFT context to calculate spectra of NiO [17] and MnO [15], but taking the self-consistent DMFT value for the average occupancy $\bar{n}_d$. The double-counting self-consistency, which can be viewed as a poor man's charge self-consistency, is necessary to stabilize the HS phase. To solve the d-shell impurity problem we have employed the continuous time (hybridization expansion) quantum Monte Carlo solver [21], which allowed us to obtain converged results even at room temperature. All calculations were done in the corundum structure with the rhombohedral (space group $R\bar{3}c$) unit cell. Throughout this Letter the compressed phase is labeled by the relative volume with respect to the experimental structure with lattice parameter $a_0 = 5.361$ Å, rhombohedral angle $\alpha = 55°17'$, and atomic coordinates Fe (0,0,0.355) and O(0.300,0,0.25). Volume reduction was achieved by scaling the lattice constant.

In Fig. 1 we show the evolution of Fe-d occupancies and the local moment under compression in the absence of magnetic LRO. We compute the *instantaneous* moment $\sqrt{\langle m_z^2 \rangle}$ and the *screened* moment $\sqrt{T\int_0^{1/T} d\tau \langle m_z(\tau) m_z(0)\rangle}$ (T is temperature) closely related to the local susceptibility [22]. In materials with a well-defined local moment, the two expressions yield similar values. At the ambient pressure we find a HS solution with a local moment of $4.6\mu_B$. Upon compression the HS phase survives down to $0.8V_0$.

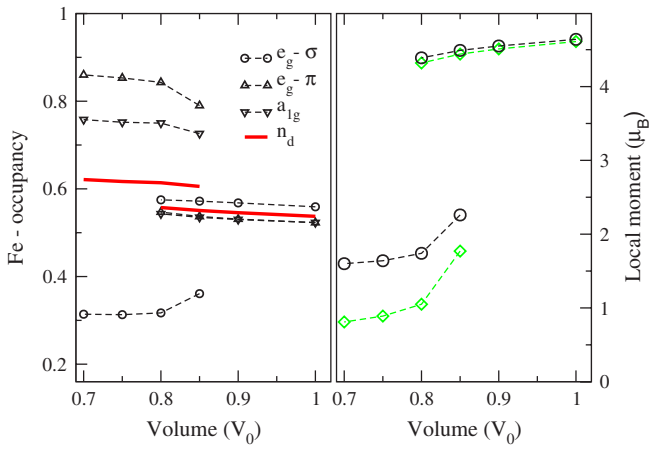

FIG. 1 (color online). Fe-d occupancies (left-hand panel) at various specific volumes in the paramagnetic (PM) state at $T = 580$ K. The thick line marks the average d occupancy per orbital. Corresponding values of the screened (diamonds) and instantaneous (circle) local moment are shown in the right-hand panel. Below this value only a LS solution characterized by a substantially reduced local moment exists. The difference between the screened and instantaneous values indicates that the LS moment cannot be viewed as a rigid object. The HS and LS solutions coexist in the 0.8–0.85V_0 range. The Fe-d orbital occupancies fit into the ionic picture of a fully spin-polarized d shell in the HS state, and an orbitally polarized d shell in the LS state. Nevertheless, the substantial e_g^σ population in the LS phase reflects a sizable covalent $p - d$ bonding (hybridization between O-p and Fe-e_g orbitals).

In Fig. 2 we show the corresponding single-particle spectra obtained with the maximum entropy method for analytic continuation [23]. In the LS phase the e_g^σ-derived bands are above the chemical potential, carrying some O-p admixture with them, which leads to charge transfer from the O-p orbitals and an increase of $\bar{n}_d$ (see Fig. 1). Relaxation of the electronic states, which compensates this charge redistribution in real material, is mimicked by the self-consistency of the double-counting term in the present scheme. Comparison to PES and inverse PES (see left-hand inset of Fig. 2) reveals a fair agreement between the theory and experiment. The computed ambient pressure HS phase is found to be an insulator with a gap of 2.6 eV. Upon compression the gap gradually shrinks due to broadening of the bands and increase of the crystal-field splitting. At the high-pressure end of the HS stability region ($0.8V_0$) the gap is reduced to a fraction of an eV. The spectra in the LS phase closely resemble the non-

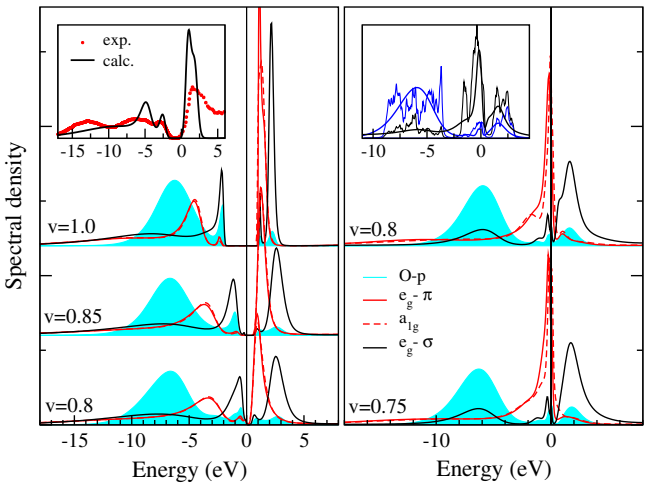

FIG. 2 (color online). Evolution of the PM single-particle spectra with pressure ($T = 580$ K). The HS solutions are shown in the left-hand panel and LS solutions in the right-hand panel. All curves are normalized to one. Left-hand inset: Comparison of experimental PES [7] and inverse PES [25] data (points) to the d spectra (solid line) with 0.6 eV Gaussian broadening to mimic the experimental resolution. Right-hand inset: Comparison of the $v = 0.8$ DMFT (smooth curves) and LDA spectra (jagged curves): the total d spectra (black lines), the total O-p spectra [gray (blue) lines].

interacting one (see the right-hand inset of Fig. 2). Orbital polarization of the t_{2g} band due to distortion of FeO_6 octahedra is seen in the LS spectra.

Unlike LDA or LDA + U, the LDA + DMFT allows opening of a gap and formation of local moments without magnetic LRO, as observed in many materials. Reducing the symmetry to allow the experimental AFM LRO we observe the following. At room temperature the HS solutions are magnetically ordered, while all LS solutions remain paramagnetic. The spin-polarized spectra (Fig. 3) show that the gap and the main spectral features are insensitive to the AFM LRO. The magnetization curves reflect increase of the exchange coupling due to shortened interatomic distances.

Our observations are summarized in the T-V phase diagram in Fig. 4. We distinguish three phases: (i) paramagnetic LS, (ii) AFM HS, and (iii) paramagnetic HS, separated by the line of Néel temperature T_N and the coexistence region of the HS and LS phases. The calculated T_N is affected by two approximations, both favoring the AFM phase. First, the lack of nonlocal spin fluctuations in DMFT, and second, the approximate form of the local Coulomb interaction, limited to Ising terms, rendering the HS local state twofold ($S_z = \pm 5/2$) instead of sixfold degenerate ($S = 5/2$). The latter is also reflected in the shape of the magnetization curves, which can be fitted with a mean-field theory based on the Brillouin function $B_{1/2}$ (see the inset of Fig. 3). Given these approximations the calculated T_N of 1600 K appears to be in reasonable agreement with the experimental value of 956 K. The effect of AFM LRO on the HS-LS transition is minor, consisting in a slight shift of the coexistence region in favor of the HS phase. Interestingly, in the vicinity of the HS-LS boundary we find that with increasing temperature the AFM LRO is not destroyed by magnetic fluctuations, but due to the collapse of the constituting moments.

Next, we discuss how a d^5 HS phase can be destabilized by increase of the crystal field (and the bandwidth) due to applied pressure. We simplify the local interaction to $\sum_{i,j,\sigma} U n_{i\sigma} n_{j-\sigma} + (U - J) n_{i\sigma} n_{j\sigma}$ neglecting the orbital dependence in order to keep the following expressions transparent. The HS gap can be estimated as

$$E_g \approx E(d^6) + E(d^4) - 2E(d^5) - W = U + 4J - \Delta - W, \quad (1)$$

where Δ is the $e_g - t_{2g}$ crystal-field splitting, W is the average of the e_g and t_{2g} bandwidths, $E(d^5)$ is the ground state energy of an ion in the HS state, and $E(d^6)$, $E(d^4)$ are the energies of the corresponding electron addition and removal states, respectively. (In charge-transfer compounds such as hematite, E_g may be substantially reduced by the presence of the ligand bands.) Similarly the energy difference between ions in LS and HS states can be estimated as

$$E(\mathrm{LS}) - E(\mathrm{HS}) = 6J - 2\Delta. \quad (2)$$

The HS state becomes unstable when either (1) or (2) becomes negative. The former is an instability with respect to transfer of an e_g electron into a t_{2g} orbital on the neighboring cation, the latter is an on-site instability with respect to redistribution of the d electrons. We adopt the

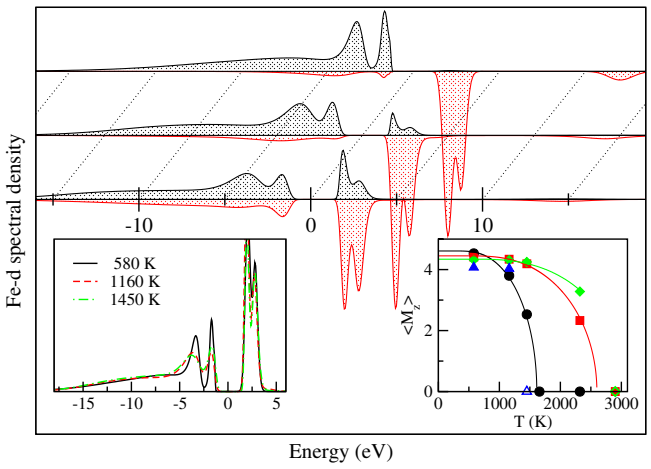

FIG. 3 (color online). Spin-polarized Fe-d spectra at the ambient pressure for 580, 1160, and 1450 K (top to bottom). Left-hand inset: The same spectra averaged over spin. Right-hand inset: The staggered magnetization versus temperature curves for $v = 1.0$ (circles, black), $v = 0.9$ (squares, red), $v = 0.85$ (diamonds, geen), and $v = 0.8$ (triangles, blue). At empty symbols only the LS solution exists. The lines represent mean-field fits.

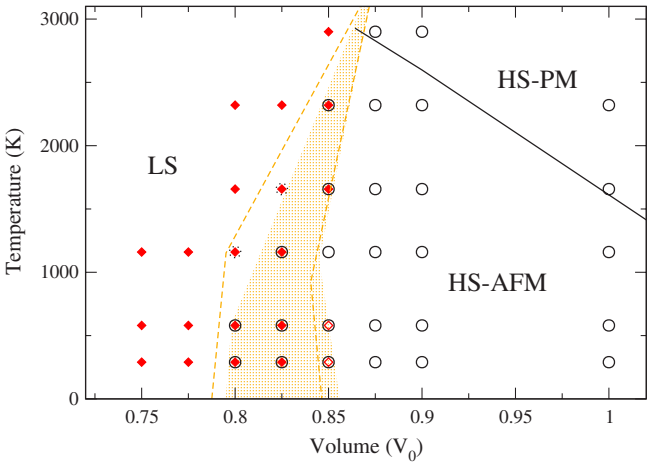

FIG. 4 (color online). Calculated V-T phase diagram of hematite. The symbols mark the actual computational results: HS state (circle), LS state (diamond). Empty diamonds mark LS solutions stable only if PM symmetry is constrained; dotted circles mark HS solutions stable only if AFM LRO is allowed. The black line shows the Néel temperature estimated from fits to $v = 1.0$, 0.9, and 0.85 data. The shaded area marks the estimated HS-LS coexistence region with PM constraint; the dashed lines mark the coexistence regime when AFM LRO is allowed.

terms *gap closing* and *local state transition* for the two types of behavior. While the gap continuously disappears as the gap closing transition is approached, in the local state transition the gap remains finite. Whether the transition in this case is insulator to insulator or proceeds through the appearance of in-gap states depends in a first approximation on U and W. We point out that analogous estimates for a two band system provide a surprisingly accurate description of the phase diagram in Fig. 2 of Ref. [24], identifying the Mott insulator-to-metal transition as gap closing and the Mott insulator-to-band insulator transition as local state transition.

Comparing the hematite spectra with the behavior of MnO [15] an obvious similarity is that the HS phase is an insulator while the LS phase is metallic. However, there are two important differences in how the transition proceeds. First, in MnO there is a continuous crossover via a sequence of intermediate states while in hematite we find a first-order transition with coexisting HS and LS solutions. Second, the HS gap in hematite shrinks practically to zero at the border line of the HS stability region while in MnO the gap does not close completely and the transition starts with the appearance of an in-gap spectral density. The latter observation leads us to the conclusion that the HS-LS–insulator-metal transition in hematite proceeds through the *gap closing* mechanism while in MnO a *local state transition* takes place as was argued in Ref. [15]. The gap closing scenario in hematite is also supported by the slope of the HS-LS phase boundary. The HS state can be destroyed by thermal fluctuations, contrary to the expectation for the local state transition where the HS state is favored at high temperature due to its higher entropy.

Finally, we briefly address the structural and volume changes [10–12]. The corundum and Rh_2O_3-II structures have similar local Fe environment, and transitions between the two were reported in other materials without significant impact on the electronic structure. Here we did not attempt to distinguish between the two structure types. Finding the electronic HS-LS–insulator-metal transition in the high-volume phase shows that the electronic transition is not conditioned by the structural transition or volume collapse. Conversely the electronic transition provides a natural explanation of the volume collapse as a consequence of emptying of the antibonding e_g^σ bands in the LS phase and corresponding strengthening of the Fe-O bonds.

In summary, we have observed a simultaneous HS-LS–insulator-metal transition in the corundum structure of hematite close to the experimental volume in the numerical results obtained by LDA + DMFT. The magnetic long-range order is found to play a minor role in the transition. We have discussed two possible scenarios, the *gap closing* and the *local state transition*, and concluded that the transition in hematite, unlike in MnO, proceeds through the gap closing mechanism. Our results are consistent with the picture of an electronically driven volume collapse.

J. K. acknowledges support of SFB 484 of the Deutsche Forschungsgemeinschaft. The calculations were performed in the Leibniz Supercomputing Center in Munich using ALPS [26]. Support by the Russian Foundation for Basic Research (Project No. RFFI-07-02-00041), Presidium of the Russian Academy of Sciences (Project No. 31, subprogram No. 3, Program No. 9) and the Swiss NSF (PP002-118866) is gratefully acknowledged.

[1] C. S. Yoo *et al.*, Phys. Rev. Lett. **94**, 115502 (2005).
[2] A. G. Gavriliuk *et al.*, Phys. Rev. B **77**, 155112 (2008).
[3] I. S. Lyubutin *et al.*, Phys. Rev. B **79**, 085125 (2009).
[4] K. Held *et al.*, Phys. Status Solidi B **243**, 2599 (2006); G. Kotliar *et al.*, Rev. Mod. Phys. **78**, 865 (2006).
[5] C. G. Shull, W. A. Strauser, and E. O. Wollan, Phys. Rev. **83**, 333 (1951).
[6] A. Fujimori *et al.*, Phys. Rev. B **34**, 7318 (1986); C.-Y. Kim *et al.*, Phys. Rev. B **66**, 085115 (2002).
[7] R. J. Lad and V. E. Henrich, Phys. Rev. B **39**, 13 478 (1989).
[8] S. Mochizuki, Phys. Status Solidi A **41**, 591 (1977); K.-H. Kim, S.-H. Lee, and J.-S. Choi, J. Phys. Chem. Solids **46**, 331 (1985).
[9] H. Liu *et al.*, Phys. Chem. Miner. **30**, 582 (2003).
[10] M. P. Pasternak *et al.*, Phys. Rev. Lett. **82**, 4663 (1999).
[11] G. Kh. Rozenberg *et al.*, Phys. Rev. B **65**, 064112 (2002).
[12] J. Badro *et al.*, Phys. Rev. Lett. **89**, 205504 (2002).
[13] L. M. Sandratskii, M. Uhl, and J. Kübler, J. Phys. Condens. Matter **8**, 983 (1996).
[14] G. Rollmann *et al.*, Phys. Rev. B **69**, 165107 (2004); M. P. J. Punkkinen *et al.*, J. Phys. Condens. Matter **11**, 2341 (1999); A. Bandyopadhyay *et al.*, Phys. Rev. B **69**, 174429 (2004); V. V. Mazurenko and V. I. Anisimov, Phys. Rev. B **71**, 184434 (2005).
[15] J. Kuneš *et al.*, Nature Mater. **7**, 198 (2008).
[16] A. V. Kozhevnikov *et al.*, J. Exp. Theor. Phys. **105**, 1035 (2007).
[17] J. Kuneš *et al.*, Phys. Rev. B **75**, 165115 (2007).
[18] Dm. Korotin *et al.*, Eur. Phys. J. B **65**, 91 (2008); S. Baroni *et al.*, http://www.pwscf.org/.
[19] V. I. Anisimov, J. Zaanen, and O. K. Andersen, Phys. Rev. B **44**, 943 (1991).
[20] A. E. Bocquet *et al.*, Phys. Rev. B **46**, 3771 (1992).
[21] P. Werner *et al.*, Phys. Rev. Lett. **97**, 076405 (2006).
[22] A. Georges *et al.*, Rev. Mod. Phys. **68**, 13 (1996).
[23] M. Jarrell and J. E. Gubernatis, Phys. Rep. **269**, 133 (1996).
[24] P. Werner and A. J. Millis, Phys. Rev. Lett. **99**, 126405 (2007).
[25] F. Ciccacci *et al.*, Phys. Rev. B **44**, 10 444 (1991).
[26] A. F. Albuquerque *et al.*, J. Magn. Magn. Mater. **310**, 1187 (2007).